Development 130, 1079-1088

doi:10.1242/dev.00333

Structural-proliferative units and organ growth: effects of insulin-like growth factor 2 on the growth of colon and skin

William R. Bennett*, Tracey E. Crew, Jonathan M. W. Slack and Andrew Ward†

Center for Regenerative Medicine, Department of Biology and Biochemistry, University of Bath, Bath BA2 7AY, UK

*Present address: UK Centre for Tissue Engineering, Room 3.446, Stopford Building, Biological Sciences, University of Manchester, Manchester M13 9PT, UK

†Author for correspondence (e-mail: a.ward@bath.ac.uk)

Accepted 18 November 2002

SUMMARY

Many epithelial renewal tissues in vertebrates are organised into structural-proliferative units. We have examined the effect of IGF2 dose on the structure of structural-proliferative units in skin and colon. The mouse strains used were the *Igf2* knockout, wild type and K:*Igf2*, a transgenic in which *Igf2* is overexpressed under control of a keratin promoter.

For both skin and colon, the histological organisation of structural-proliferative units was unaltered with increasing IGF2 dose, although there was a higher fraction of dividing cells in the proliferative compartment. In the colon an increase in IGF2 dose increases the overall area of the epithelium. This is due to an increase in the number of crypts with no change of cell size or of crypt area. Growth stimulation appears to be due to a reduction in the duration of crypt fission. The conclusion is that the IGF2 pathway can stimulate the multiplication of colonic crypts independently of stimulating increased cell proliferation.

The results for the skin are consistent with this. An increase of IGF2 dose increases the proportion of dividing cells in the basal layer, the thickness of the epidermis and the total area of the epidermis.

By comparison with *Drosophila*, these results show no effects on cell size, but do show the possibility of inducing disproportionate growth. These differences may represent properties of the SPU organisation that is characteristic of vertebrate tissues.

Key words: Insulin-like growth factor 2 (IGF2), Growth, Size, Proportion, Intestinal crypts, Epidermis, Structural-proliferative units (SPUs), Proliferating cell nuclear antigen (PCNA)

INTRODUCTION

An animal consists of several distinct parts, or organs. Each of these grows enormously between the period of organ specification in the embryo, and the fully grown adult. In the case of a human embryo, from limb bud stage to adult, the expansion is of the order of 10^9-fold. This fact raises a number of questions about the control of the process (Goss, 1972; Slack, 1996; Raff, 1996). What determines the rate of growth? How is the growth of one organ coordinated with the growth of other parts? How is it related to the growth of the whole animal? Why does growth stop?

Growth can be considered at various levels: subcellular, cellular and organismal. At the subcellular level, there is the molecular biology of the various component processes: the cell division cycle, the action of growth factors or the mechanism of apoptosis. These are all key processes that have been the subject of much recent research. But most of the information comes from studies on tissue culture cells. Although very convenient for molecular biology, cells in culture are not a good model for the growth of tissues in the body, as they are typically homogeneous monocultures showing exponential growth. In vivo, exponential growth is rarely found and most cell division occurs at particular sites within a defined three-dimensional tissue architecture. Furthermore, in vivo, most tissues consist of multiple cell types, the production and turnover of which needs to be coordinated.

Organs are not homogeneous masses of similar cells. They normally consist of microanatomical structural units and these are often also units of cell proliferation control (Potten, 1978; Potten, 1998). This may be demonstrated by examples in which the clonal organisation of structural units can be visualised, such as mouse aggregation chimeras between different strains, X-chromosome inactivation mosaics or mutagenesis studies (Gordon et al., 1992). If a structural unit is fed by a single stem cell, then it will necessarily appear monoclonal under conditions where individual clones can be experimentally distinguished. Monoclonality is seen, for example, in the intestinal crypts (Ponder et al., 1985; Winton et al., 1988), cell patches in the epidermis (Potten, 1974; Jones et al., 1995), endometrial glands (Jiang et al., 1996), terminal ductal-lobular units in the breast (Tsai et al., 1996) and cell columns in the adrenal cortex (Weinberg et al., 1985). In fact, such observations do not preclude structural units from containing more than one stem cell, because random elimination of individual cellular lines of descent can also lead to monoclonality (Schmidt et al., 1988). Histological structural

units that are also units of cell proliferation will be referred to here as ‘structural-proliferative units’ or SPUs.

Significant growth of an organ cannot occur without an increase in the number or size of SPUs, so the regulation of the multiplication of SPUs is a central and crucial issue when considering the control of growth generally. In general, the number of SPUs increases during the growth of the animal but achieves a steady state with minimal turnover once full size is attained. For example, the number of nephrons in the kidney stops increasing about 40 days after birth in rats (Canter and Goss, 1975), while in the colon the fission of crypts declines to a steady state of 1-2% by 8-10 weeks (Maskens, 1978; Cheng and Bjerknes, 1985). The ability to repair damage to tissues and organs is dependent on whether the ability to produce new SPUs is retained, and this is associated with, although not identical to, the pattern of normal multiplication. For example new nephrons cannot be produced in the rat kidney beyond about 50 days, not much longer than the normal growth period (Canter and Goss, 1975), while new intestinal crypts can arise at any stage in response to irradiation or other damage (Cairnie and Millen, 1975). So not only is the control of the number of SPUs during growth central to normal growth control, but it is also crucial for the prospects of repair to damaged tissues and organs.

There are very few ways known in which it is possible experimentally to vary the relative growth of parts during embryogenesis. The majority of cases where this has been achieved have involved the insulin/insulin-like growth factor (IGF) signalling system in *Drosophila*, where insulin-like ligands stimulate their tyrosine kinase receptor, and thereby activate PI3 kinase, protein kinase B and S6 ribosomal protein kinase (Oldham et al., 2000; Leevers, 2001). In vertebrates, the homologous pathway involves three ligands (insulin, IGF1 and IGF2) interacting with at least two signalling receptors (IR and IGF1R), with effects on growth mediated by IGF1R (Efstratiadis, 1998). In humans, IGF2 overexpression is associated with disproportionate overgrowth in Beckwith-Weidemann syndrome (Ward, 1997). Although rare, by analogy with the discovery of tumour suppressor genes in rare familial cancers, a better understanding of such growth conditions is likely to have an importance much greater than is suggested by the relatively small proportion of affected individuals.

In the present work, we have studied the effects of the IGF2 pathway in a mammalian system. We have used three strains of mice differing in their IGF2 status to investigate the relationship between the multiplication of the SPUs within particular organs and the growth of the organ as a whole. We have examined two contrasting types of SPU: in the colon and in the epidermis of the skin. In the colon, each crypt represents a single SPU. The stem cells are located at the base, the transit-amplifying cells in the lower part of the crypt and the differentiating cells in the upper part. Cells are produced in the basal region, progress up the crypt and become shed into the lumen of the colon (Wright and Alison, 1984). In the epidermis, an SPU consists of a stem cell together with its progeny (Potten, 1974). The stem cells and the transit cells lie in the basal layer, while cells in suprabasal layers are postmitotic and differentiating. They progress upwards and eventually lose their nuclei and become shed from the exterior surface of the skin (Watt, 1998).

When the IGF2 dose to either of these systems is altered, the number of cell divisions is altered. We were interested to know whether an increase in cell division affects the growth of the organ or simply drives cells faster through their differentiation pathway, speeding up the cell turnover. Furthermore, if growth is affected, does this arise from a change in size of SPUs or in the total number of SPUs, or by some combination of both effects? Our results show that IGF2 dose does affect growth and it does so by controlling the number rather than the size of SPUs. The IGF2 pathway must therefore, in some way, control the multiplication of the SPUs, as well as affecting the cell division cycle itself.

MATERIALS AND METHODS

Mice

All mice were housed under standard conditions and experienced 13 hours light:11 hours darkness (lights on 06:30-19:30, including 30 minute periods of dim lighting to provide false dawn and dusk), a temperature of 21±2°C and relative humidity of 55±10%. Food (CRM formula; Special Diets Services, Witham, Essex, UK) and water was freely available.

For the present study two strains of mouse were used, with over- and under-expression of IGF2, and were compared with the wild type. K:*Igf2* is a transgenic containing an *Igf2* gene driven by a keratin promoter (Ward et al., 1994). The full designation is *Tg(Igf2)B1Ward*, and it has previously been referred to as ‘Blast’. There is overexpression of IGF2 in several tissues, including the skin, colon and endometrium. The mice show overgrowth of the affected organs and the DNA content of the listed organs is increased, showing that the cell number is increased and that the enlargement is not simply due to an increased content of water or extracellular materials. The *Igf2* knockout shows a considerable growth deficit during embryonic life. Newborns are about 60% of wild-type size and remain small throughout life. Although small, the mice are otherwise normal and the relative proportions of body parts are conserved (De Chiara et al., 1990). Control animals used in the study were wild-type littermates of the *Igf2* knockout and K:*Igf2* mice.

Igf2 knockout and K:*Igf2* hemizygous transgenic male mice were crossed to non-transgenic F_1 (C57BL6×CBA) females. The imprinted nature of the *Igf2* locus means that paternal transmission of the disrupted knockout allele results in heterozygous *Igf2* knockout offspring with a growth retardation phenotype that is essentially indistinguishable from homozygotes. The K:*Igf2* transgene acts in a dominant manner, but cannot be transmitted maternally because of phenotypic effects on the uterus rendering transgenic females subfertile. The results on the number, size and labelling indices of the SPUs are presented in terms of ‘IGF2 dose’, which we know increases in the series: *Igf2* knockout<wild type<K:*Igf2*.

In addition, we have used H253 mice, a strain that carries several *lacZ* genes on the X chromosome in the region subject to X-inactivation (Tan et al., 1993), to visualise the clonal makeup of tissues. H253 transgenic males were crossed to non-transgenic F_1 (C57BL6 × CBA) females, and female offspring were tested for the presence of the X-linked transgene by β-galactosidase staining of earclips. Transgenic females from these crosses were obligate hemizygotes, giving mosaic expression of the transgene. Expression of the X-linked transgene was ubiquitous in epidermis and colon crypts from homozygous females or males (data not shown).

Genotyping

Igf2 knockout samples were distinguished from wild type by multiplex PCR using primers Igf2-91 (5′-CTGTGAGAACCTTCC-AGCCTTTTC-3′), Igf2-92 (5′-GTGAGAGACCAGTGCGGAATAA-

TC-3′), Neo-80 (5′-CATCGCCTTCTATCGCCTTC-3′) and Igf2-95 (5′-CATGCCAGCAAGGATAGTCA-3′). These primers generate a 400 bp product from the *Igf2* knockout disrupted gene and a 640 bp product from the intact wild-type gene. Ear clips from animals to be tested were boiled for 10 minutes in 1 ml freshly prepared 50 mM NaOH, then neutralised by the addition of 50 μl 1 M Tris HCl (pH 8.0). This mixture (1 μl) was added to 24 μl reaction mix to give a 25 μl reaction containing 75 mM Tris HCl (pH 9.0), 20 mM $(NH_4)_2SO_4$, 0.01% Tween-20, 3 mM $MgCl_2$, 250 μM dNTPs, 1U *Taq* polymerase and 150 nM each primer. Thirty-six reaction cycles were carried out, each consisting of 60 seconds denaturation at 95°C, 60 seconds annealing at 60°C and 60 seconds extension at 72°C.

K:*Igf2* samples were distinguished from wild type by slot blotting. Genomic DNA was prepared from tail biopsies as previously described (Ward et al., 1997) and approximately 10 μg was denatured by addition of an equal volume of 1 M NaOH and incubation for 10 minutes at room temperature. Denatured DNA was loaded onto nylon membrane (Hybond-N+, Amersham) pre-incubated in 0.5 M NaOH and placed in the slot-blot apparatus (Flowgen). The filter was neutralised, air-dried and UV crosslinked, then probed using a radiolabelled fragment corresponding to exons 4-6 of the *Igf2* gene (Ward et al., 1994). The K:*Igf2* transgene has more than 25 copies of this region of the *Igf2* gene; hence, the probe readily distinguishes between endogenous and transgene-related signal.

Histological analysis

The histological analysis was carried out at three developmental stages: neonatal, when SPUs are newly established, about 2 weeks postnatal, when whole organism growth is still rapid, and about 3 months, when whole organism growth is slowing. Some studies focused more closely on the crucial 2-4 week postnatal period.

Sample collection

Samples were collected at 0.5, 13.5 and 83.5 days post-partum (neonate, 2-week- and 12-week-old mice). Mice were killed by cervical dislocation and samples dissected from the mid-portion of the colon and from the dorsal skin roughly in the centre of the back. Samples were fixed for 24 hours in 10% formaldehyde in PBS, or in Zamboni's fixative [85 mM sodium phosphate buffer (pH 7.3), 0.85% paraformaldehyde, 15% saturated picric acid], then embedded in paraffin wax, and sections cut at 7 μm. Conventional Haematoxylin and Eosin (H&E) staining was performed for nuclear counting.

Total crypt number analysis

For analysis of colon crypt density, crypt fission and water content, samples were collected at 13.5, 20.5 and 27.5 days post-partum (2-, 3- and 4-week-old mice). The entire colon was dissected open in PBS, the contents washed out and the colon squashed flat between glass slides. The lumenal surface was examined under a dissecting microscope and photographed using a digital SPOT-RT camera (Diagnostic Instruments) at 8× magnification. Randomly chosen areas of the distal, mid and proximal colon were also photographed at 100× magnification. SPOT V3.3 software was used to measure the surface area of the entire colon at low power and to count the number of crypts across randomly selected fields (though note that it was necessary to reject fields containing folded tissue, where it was impossible to accurately count crypts across the entire field) of the distal, mid and proximal regions sampled at high magnification.

Crypt fission analysis

Regions of dissected mid-colon were fixed and processed through to H&E stained sections as above, then examined for fissioning crypts. Crypts were only counted if they could clearly be seen to extend from the base to the lumenal surface, as evidenced by a lumenal brush border. Fissioning crypts were so designated if a region of bifurcation was visible in the lower 75% of the crypts, eliminating false positives caused by two mature adjacent crypts overlapping slightly near their tops in the plane of section. To reduce sampling bias, one person scored all of the samples in a blind fashion. It should be noted that this method is relatively simple and allowed for a robust comparison between samples from animals of different genotypes. A more definitive fission index might be derived using microdissected colon tissue (Goodlad, 1994).

Water content analysis

Part of the dissected colon was accurately weighed and then dessicated for 6 days in a 65°C oven to remove water content. It was then re-weighed and the water content determined.

β-galactosidase staining

H253 colon samples were fixed in 100 mM phosphate buffer (pH 7.4), 4% paraformaldehyde, 2 mM $MgSO_4$ and 5 mM EGTA for 30 minutes at 4°C. Tissues were then rinsed and incubated for 30 minutes at room temperature in the same solution minus the paraformaldehyde, then rinsed and incubated for 5 minutes at room temperature in 100 mM phosphate buffer (pH 7.4), 2 mM $MgCl_2$, 5 mM $K_3Fe(CN)_6$, 5 mM $K_4Fe(CN)_6$, 0.01% sodiumdeoxycholate and 0.02% NP-40. Tissues were then stained overnight at 28°C in the same solution containing 1 mg/ml X-Gal. Stained colon samples were refixed overnight in 10% formaldehyde in PBS, wax embedded and sectioned. Sections stained with X-Gal were counterstained with nuclear Fast Red.

Epidermal wholemounts

Dorsal mouse skin was removed from the carcass and pinned out. Fur was removed using Immac hair removal cream (Reckitt Benckiser), followed by gentle scraping with a blunt scalpel. The denuded skin was cut into 1.5 cm pieces, washed in PBS and incubated overnight in DMEM containing 2.5 mg/ml Dispase II (Boeringher) at 4°C. The epidermis was then carefully separated from the underlying dermis using a scalpel blade, washed in PBS and fixed for 5 minutes in 10% formaldehyde in PBS and stained for β-galactosidase as above. Epidermal wholemounts were mounted under coverslips and photographed using brightfield illumination on a Leica DMRB equipped with a digital SPOT-RT camera.

Antibody staining

Anti-proliferative cell nuclear antigen (PCNA) antibody was used to mark proliferating cells. Slides from samples fixed in formaldehyde were dewaxed and rehydrated, then placed in a domestic pressure cooker containing boiling 10 mM sodium citrate buffer pH 6.0 and pressure cooked for 60 seconds to retrieve the antigen. Slides were washed for 10 minutes in PBS with 0.1% Tween-20 (PBST), then endogenous peroxidase activity was quenched by incubation in 3% H_2O_2 (wt/vol) in tap water for 5 minutes, followed by 0.5% H_2O_2 in methanol for 30 minutes. Slides were washed three times for 10 minutes each in PBST, then blocked and incubated with primary and secondary antibodies using the Vector Mouse-on-Mouse (MOM) kit (Vector), according to the manufacturers instructions. The primary antibody (anti-PCNA, monoclonal PC10, Dako) was used at a concentration of 1:500. After application of secondary antibody, streptavidin-horseradish peroxidase complex (ABC kit, Vector) and diaminobenzidine (DAB kit, Vector) were used for detection. Slides were then counterstained with nuclear Fast Red, dehydrated and mounted.

Cell counts and proliferative index measurement

In the skin, an unfurrowed region of epidermis containing no hair follicles was aligned horizontally along a 300 μm frame at ×400 magnification and all epidermal nuclei were counted. In the colon, crypt heights were counted only if the crypts could clearly be seen to extend from the base to the brush border at the lumenal surface. Crypts in cross-section were counted only if they appeared circular to reduce counting errors due to oblique sections.

As proliferating cells were not found above the basal layer, the

proliferative index (PI) in transverse skin sections was taken to be the ratio of PCNA-positive cells to the total number of cells in the basal layer only. In the crypts, the PCNA index was taken to be the ratio of PCNA positive cells to the total number of cells in the crypt.

The use of cell-cycle-related antigens as a measure of proliferative index has well-documented pitfalls (Ezaki, 2000). In this study, we have attempted to overcome these variables by using a standardised immunohistochemical regime throughout, and by all sections being scored by one person. This has allowed us to measure relative differences in PCNA staining between genotypes with confidence, but the data should not be taken as an accurate measure of the actual number of proliferating cells in the samples.

Apoptotic index measurement

Wax sections (7 μm) from 3-week-old mid-colon samples were processed for TUNEL staining using the ApopTag Red in situ apoptosis detection kit (Intergen), according to the manufacturer's instructions. Apoptotic nuclei were stained with rhodamine, and nuclei were counter-stained with DAPI. As for crypt height measurement, crypts were only selected for scoring if they extended longitudinally from base to lumen, with the brush border visible. At least 50 such crypts were counted from each animal, and the number of apoptotic nuclei in these crypts was counted. Apoptotic rhodamine signal was checked for veracity by comparison with the blue (DAPI) channel (to ensure that a cell nucleus was present) and by comparison with the green channel (to eliminate false positives due to auto-fluorescence). The apoptotic index was derived by placing the number of apoptotic nuclei over the total number of cells scored (number of crypts counted × height × 2; where height was the number of cells on one side of the crypt, counted from base to top, and a factor of 2 has been used to estimate the number of cells visible in the whole crypt).

As with PCNA staining, the limitations of TUNEL staining are well documented, but largely centre around false positives rather than lack of sensitivity. The use of sections, rather than examining whole crypts has also been carefully compared and the errors introduced are fairly consistent (Potten and Grant, 1998). The figures given for apoptotic indices should therefore not be considered as true measures of the levels of cell death, but rather as useful metrics to make comparisons between genotypes.

Statistical analysis

The Kruskal-Wallis test was applied to data to test for differences between the three genotypes at each timepoint. This one-way analysis of variance test does not assume a normal distribution in the data. The level of significance was set at $P<0.05$.

RESULTS

SPU structure

The SPU structure of both of the tissues under study can be seen by examination of clonally labelled mouse strains such as the H253 (Tan et al., 1993). This carries a multiple *lacZ* insertion on the X chromosome. In female hemizygotes, the β-galactosidase is only expressed in half the cells because of the phenomenon of X-inactivation, which occurs early in embryonic life and is thereafter heritable in lineages of cells (Lyon, 1961). As expression of the enzyme is a heritable feature at the cellular level, staining for β-galactosidase can reveal the clonal organisation of tissues. Fig. 1 shows a frozen section of colon and whole-mount preparation of epidermis from H253 female hemizygotes. In the case of the colon, the crypts are either fully labelled or unlabelled. Although it is thought that there are several functional stem cells feeding each crypt, this indicates that at some stage all the stem cells were derived from a single progenitor cell. This result is similar to previous studies of crypt clonality using aggregation chimeras (Ponder et al., 1985). In the case of the epidermis, the SPU arrangement is less regular and without clear anatomical boundaries, but it can be seen that the blue and white cells are not interspersed in a 'pepper and salt' manner, but rather the tissue is made up largely of coherent clusters of blue or white cells. The few individual blue cells are thought to be migratory types such as macrophages. As this is a wholemount seen from the surface, each patch is viewed through the full thickness of the epidermis and is therefore a column of cells. We believe that each patch represents an SPU fed by a single stem cell in the basal layer, or a coherent group of a few such SPUs (Watt, 1998).

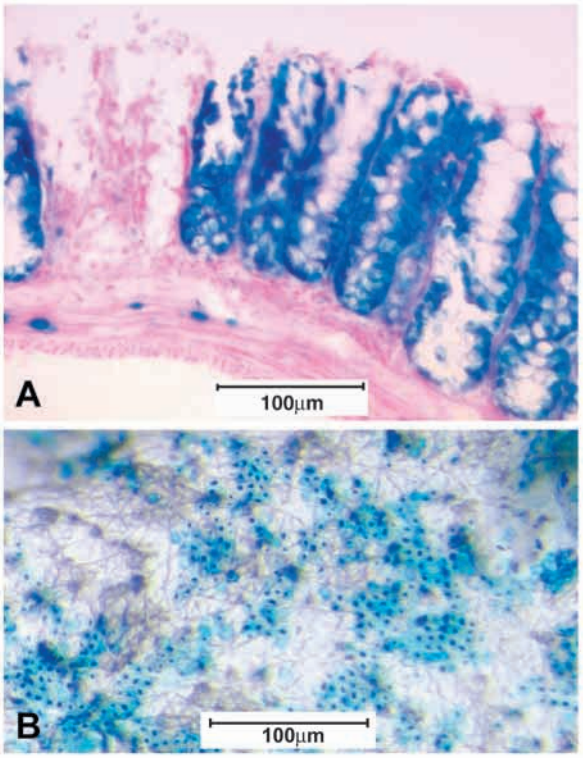

Fig. 1. Visualisation of SPUs in H253 female hemizygotes. Specimens are stained with X-Gal to reveal β-galactosidase-positive (blue) cells. (A) The colon at 12 weeks of age, showing monoclonality of crypts. (B) The skin, epidermal wholemount viewed from exterior surface showing columns of blue cells extending through the epidermis.

Colon

It is already known that IGF2 is ectopically expressed throughout the gut epithelium of the K:*Igf2* mouse, and that the colon becomes larger than normal (Smith et al., 2000). It has a higher DNA content, indicating that the difference is based on the presence of more cells rather than just water or extracellular material (Ward et al., 1994). But it was not known to what extent the increase in cell number was in the epithelium and to what extent in the connective tissues. Nor was it known how the increased overall size related to the SPU structure of the epithelium. We have made a detailed analysis to examine this question.

We measured water content in the present study and found that that the ratio of wet to dry weight was, as expected, constant in the three strains (results not shown). In order to gain a comparative estimate of overall epithelial area, we measured the total lumenal area of the colon of knockout, wild-type and K:*Igf2* strains during the rapid growth phase of 2-4 weeks postnatal. The results show a substantial effect of IGF2 dose. By 4 weeks of age, the K:*Igf2* colon area is almost double that of the knockout (Fig. 2A). In the case of the knockout to wild type difference, this is consistent with the overall size of the animals. In the case of the wild type to K:*Igf2* difference, it arises from a disproportionate growth of the colon relative to the whole body, with the proximal colon showing a relatively greater increase in surface area.

Does this difference arise from larger crypts, more crypts, or a mixture of both effects? To answer this, we examined the size of crypts. In this context it is the size in the plane of the epithelium that is important and, as we did not see any indication of a change in cell size, this was measured by counting the number of cells around the circumference of the crypts. The results showed rather little difference: the K:*Igf2* crypt circumference was a little larger than the others at 2 weeks but this difference was lost by 12 weeks (data not shown). This shows that the increase of area with IGF2 dose is not due to an increase in crypt size. It might, in principle, be due to an increase in crypt number, or to a larger amount of space between crypts. In order to resolve this, the total number of crypts was counted as described in the Materials and Methods. Comparison of these results with the area measurement shows that indeed virtually all of the area increase is attributable to an increase in crypt number (Fig. 2B).

Of course, crypt size may change in the other axis, perpendicular to the surface. To examine this, the crypt heights were measured for the three strains and the results are shown in Fig. 2C. There is an increase in crypt height with time for all strains, and also an effect of IGF2 dose which is much stronger at 2 weeks than at 12 weeks. At 2 weeks, the K:*Igf2* mice show crypt heights almost double the knockouts, while by 12 weeks all the crypts have increased in height and the difference between K:*Igf2* and the others is only about 15%.

So driving extra cell production with IGF2 does increase the crypt size, but only temporarily, and not in the axis that will affect the total area of the epithelium. It is known that the crypt number increases during normal development by binary fission, with the division commencing at the crypt base (Maskens, 1978; Cheng and Bjerknes, 1985; Bjerknes, 1986) (Fig. 3). We measured the fission index during the critical growth phase and found the overall mean index to be 8.7%, with no significant difference between the three strains at any of the time points examined (Fig. 4A). There may be a reduction in the index after 2 weeks, but as this is a difficult parameter to measure accurately we cannot be confident about this. If the log of crypt number is plotted against time (Fig. 2B), only the *Igf2* knockout data produce a straight line, suggesting uniform exponential growth. In this case the doubling time is 12 days, so the 8.7% fission index would lead to an approximate estimate of fission duration of 1.04 days or 25 hours. For the other two strains there is no straight line relationship: as may be seen in Fig. 2B, the crypt numbers increase at a faster rate than exponential, indicating that the presence of IGF2 accelerates the crypt fission rate during the rapid growth phase. For the 3-4 week interval the doubling time is about 7 days for both strains, and so the 8.7% mean fission index would predict a duration of fission of approximately 0.61 days or 15 hours. These estimates are not very accurate because of the variation in crypt fission index between individuals and indeed ANCOVA analysis of the slopes of the semi-log plots do not show significant differences (P>0.05). However the indication is that the presence of IGF2 drives faster crypt fission by reducing the time taken for each crypt to divide.

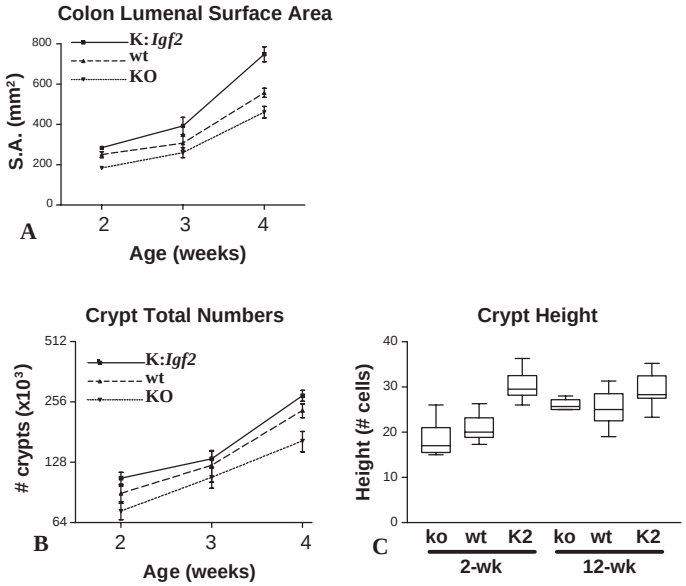

Fig. 2. Growth of the colon in *Igf2* knockout, wild-type and K:*Igf2* mice. (A) Lumenal area measured at 2-4 weeks of age. (B) Semi-log plots of crypt numbers measured at 2-4 weeks of age. (C) Comparison of crypt heights measured at 2 weeks and 12 weeks of age (K:*Igf2* samples indicated by K2). Each animal was sampled in triplicate and results averaged (medians indicated by horizontal bars, interquartile range by boxes and full range by vertical capped bars); n≥6 for each genotype tested. Kruskal-Wallis test for significance: 2-week (columns 1-3) P<0.0001; 12-week (columns 4-6) P=0.0284.

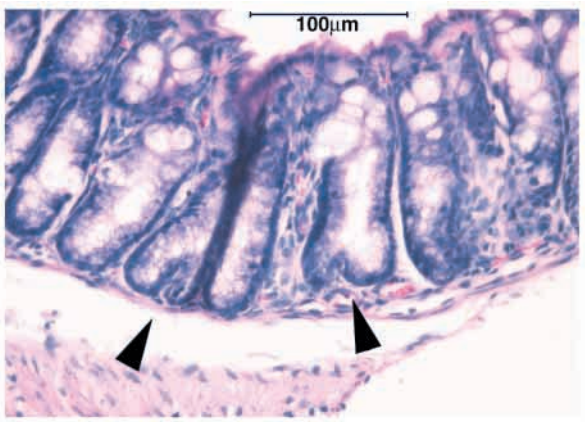

Fig. 3. Crypt fission in the colon (the sample shown is wild type, 2-week postnatal). Bifurcating crypts are indicated by arrowheads.

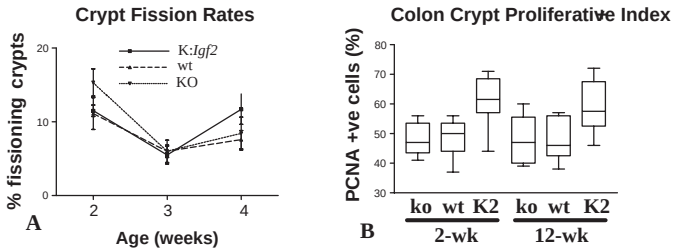

Fig. 4. Colon crypt expansion in *Igf2* knockout, wild-type and K:*Igf2* mice. (A) Crypt fission rates at 2-4 weeks of age. (B) Proliferative index measured at 2 weeks and 12 weeks of age (K:*Igf2* samples indicated by K2). At least 6 crypts were sampled in each animal and the results averaged (medians indicated by horizontal bars, interquartile range by boxes and full range by whiskers); $n \geq 6$ for each genotype tested. Kruskal-Wallis test for significance: 2-week (columns 1-3) $P=0.0069$; 12-week (columns 4-6) $P=0.0293$.

Crypt fission must be driven by an increase in cell numbers, although cell production feeds the turnover of the epithelium, as well as increases in size. Fig. 5A-D shows the PCNA labelling pattern of the three strains, and in Fig. 4B a graphical representation of the PCNA index at 2 weeks and 12 weeks. It is exceedingly difficult to calculate absolute net cell production rates for epithelia in situ (Wright and Alison, 1984) and we have not attempted to do this. But it is likely from the direct comparison of the PCNA indices that K:*Igf2* is producing more cells than the other two strains, and that the difference is present both at 2 weeks, during rapid growth of the organism, and at 12 weeks, when growth is slowing down. So the rate of crypt number growth increases from knockout to wild type, while the proliferative index increases from wild type to K:*Igf2*. This suggests that the main effect of the normal IGF2 level may be to suppress cell death, while an increase above normal increases overall cell turnover.

Apoptosis in colonic crypts was measured by TUNEL staining and compared between K:*Igf2* and wild-type mice at three weeks of age (Fig. 5E,F). *Igf2* knockout crypts were excluded from this analysis because knockout crypts were indistinguishable from those of wild-type animals, both in terms of height (Fig. 2C) and proliferation indices (Fig. 5A-D). For K:*Igf2* mice (n=5), the mean apoptotic index was 0.24% (range, 0.06-0.47%), and for wild type (n=3), the mean apoptotic index was 0.34% (range, 0.17-0.46%). Thus, there is no significant difference in the steady-state level of apoptosis between the two genotypes. This should be considered in light of the fact that the baseline level of apoptosis in the large intestine is very low, and that our figures fall within the range given for previously published data (Potten, 1998; Potten and Grant, 1998). It should be further borne in mind that apoptotic cell clearance may occur in less than 2 hours, and that very small (and hence difficult to measure) shifts in the apoptotic index could result in large changes in cell flux.

In conclusion, it is clear that IGF2 is not necessary to maintain the colonic crypt structure because the organisation is normal in the *Igf2* knockout mouse. But an increasing IGF2 dose does drive more cell division in the crypts. Some of the new cells end up contributing to new growth, as opposed to cell turnover, and this takes place by reducing the duration of crypt fission such that the number of crypts, and thus the total area of the epithelium increases.

Skin

The K:*Igf2* mouse has the IGF2 gene driven by a bovine *keratin 10* promoter that is active in the suprabasal layers of keratinocytes (Smith et al., 2000). Although the excess IGF2 is not expressed in the basal layer itself, the protein evidently reaches the basal layer as in all three strains of mice this is the only layer containing dividing cells. There is clearly an increase in total skin area with IGF2 dose. For knockout and wild type the increase is proportional to the surface area of the animal. For the K:*Igf2*, the mice are normal size but the skin is distinctly wrinkled (Ward et al., 1994). This means that the

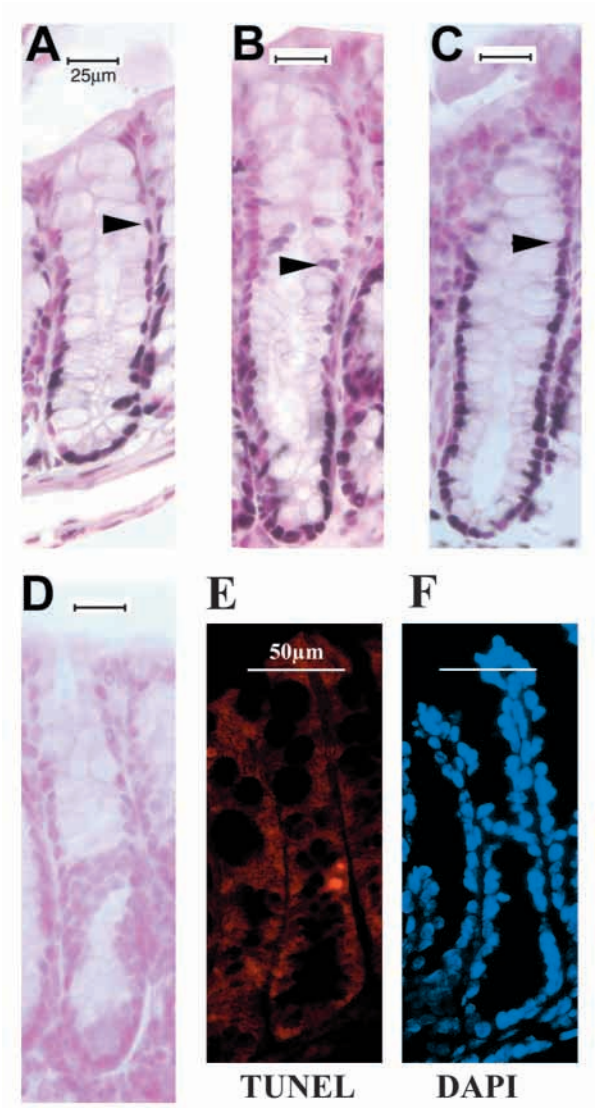

Fig. 5. PCNA and TUNEL labelling of colonic crypts. (A-D) PCNA staining of *Igf2* knockout (A), wild type (B), K:*Igf2* samples (C) and. negative control (D; wild-type sample with primary antibody omitted). The proportion of the crypt that is PCNA positive is greater in the K:*Igf2*. The knockout crypt shown is quite short but within the normal range of sizes. Scale bars: 25 μm. Arrowheads indicate the upper limit of PCNA-positive cells. (E,F) Crypt from a wild-type animal viewed for TUNEL (E; showing a single apoptotic cell) and DAPI (F, showing all nuclei) staining. Scale bars: 50 μm.

skin is definitely increased in area but it is not possible to make an accurate quantitative estimate.

The main difference between the three strains is that the total skin thickness is greatly increased in the K:*Igf2s*. This is apparent both from the histological sections (Fig. 6) and from the total epidermal cell counts (Fig. 7A). The PCNA labelling shows that dividing cells are confined to the basal layer in all three strains (Fig. 6). There is some tendency for the labelling index to be higher with IGF2 dose (Fig. 7B), although clear statistical significance is only reached by the 2 week data, corresponding to the maximum growth rate of the organism. So, as in the colon, the cell division is confined to the normal location, and there is some increase in height of the SPUs. Because it is not possible to visualise the SPUs, we cannot be sure that the number has increased, although this would be consistent with the increase of overall skin area.

The number of cells in the basal layer were counted along a fixed distance for all three genotypes as the denominator for the PCNA index and showed no significant difference (data not shown). This supports a lack of change in cell size with IGF2 dosage.

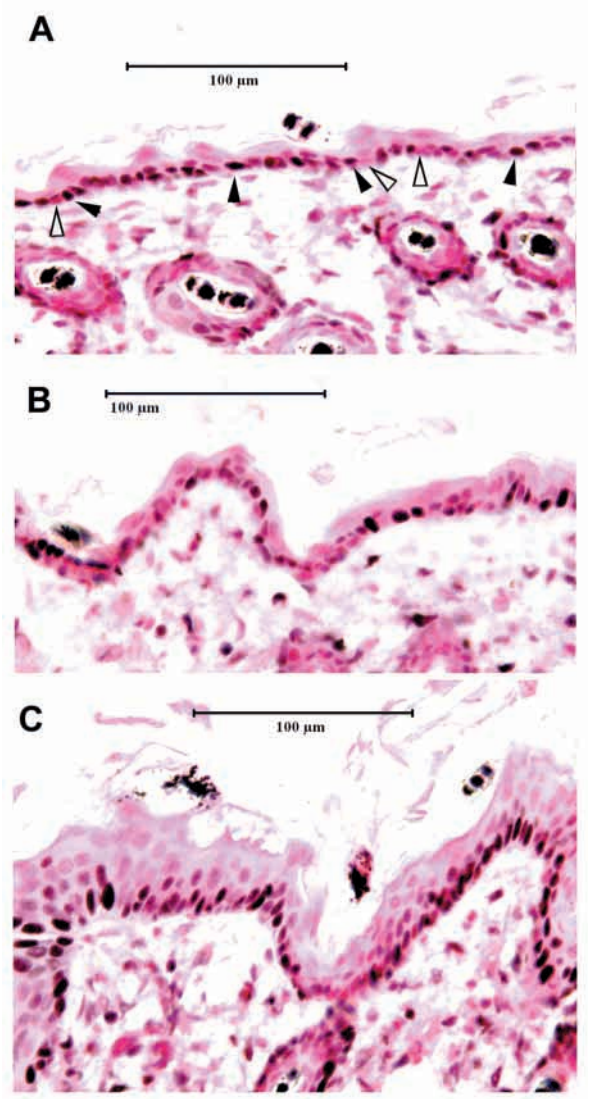

Fig. 6. PCNA labelling of skin in transverse section from *Igf2* knockout (A; some of the PCNA positive cells are indicated by black triangles and some of the PCNA negative cells by white triangles), wild-type (B) and K:*Igf2* (C) mice.

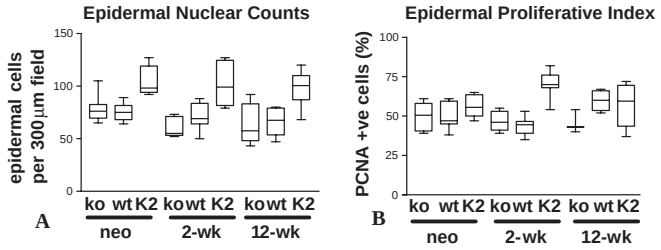

Fig. 7. Epidermal expansion in *Igf2* knockout, wild-type and K:*Igf2* mice. Mice were sampled on the day of birth (neo), at 2 weeks (2-wk) and at 12 weeks (12-wk) of age. (A) Epidermal cell number (nuclear counts). Each animal was sampled in triplicate and results were averaged (medians indicated by horizontal bars, interquartile range by boxes and full range by vertical capped bars); $n \geq 6$ for each genotype tested. Kruskal-Wallis test for significance: neonatal (columns 1-3) $P=0.0039$; 2-week (columns 4-6) $P=0.0002$; 12-week (columns 7-9) $P=0.0015$. (B) Epidermal proliferative index. Each animal was sampled in triplicate and results were averaged (medians indicated by horizontal bars, interquartile range by boxes and full range by vertical capped bars); $n \geq 5$ for each genotype tested. Kruskal-Wallis test for significance: neonatal (columns 1-3), $P=0.2837$ (not significant); 2-week (columns 4-6) $P=0.0007$; 12-week (columns 7-9) $P=0.0693$ (not significant).

DISCUSSION

IGF2 increases the number of SPUs

The object of this investigation was to find what happens to the structural-proliferative units when cell production in a renewal tissue is increased or decreased. We have compared normal mice with *Igf2* knockouts and with IGF2-overexpressing transgenics. An important conclusion is that IGF2 does not affect the gross organisation of the SPUs, as in all three lines the overall structure is normal and we do not see dividing cells out of their normal position in the basal layer of the skin or the lower region of the colonic crypt. The PCNA labelling data show that when the IGF2 dose is increased above normal, the number of cell divisions is increased, probably through an increase in size of the transit amplifying cell compartment. Because there is no existing method to measure a true flux to cell death, we have not attempted in this study to measure absolute net cell production rates. But it is thought that the stimulation by IGF2 is not just due to an increase of cell division but also to a reduction of apoptosis, which can account for a significant fraction of cell turnover in renewal tissues. This may be particularly important where IGF2 levels are lower than normal (Petrik et al., 1999; Burns and Hassan, 2001).

We were interested to know whether these changes in cell division affected the growth of the organ or simply drove cells through their differentiation pathway at a different rate. The results show that in both colon and skin there is an effect on overall growth. In this context, it is appropriate to consider what fraction of cell production is feeding growth compared with that feeding renewal. In the case of the colon this may be

estimated from published data (Wright and Alison, 1984). The figures show some variation with position, but, as the crypts are smaller in regions of lower cell production, the estimated cell number doubling (i.e. turnover) times do not vary greatly and are in the range 1.5-3.3 days, with a mean of 2.4 days. There is little effect of age of the mouse up to 70 days postnatal. For our wild-type mice, the minimum time for crypt number to double is about 7 days at 3 weeks postnatal, indicating that the normal situation involves about one third of cell production being devoted to growth and two thirds to turnover. On the basis of the PCNA index, the cell division rate appears similar in *Igf2* knockout and wild type but the crypt number doubling time falls from 12 days to a minimum of 7 days, indicating a shift from about 20% to 30% of cell production devoted to growth. This shift could be due to a suppression of cell death as this is a function previously attributed to IGF2 in both normal and hyperplastic growth states (Christofori et al., 1995; Burns and Hassan, 2001). In our analysis of wild-type and K:*Igf2* mice, no significant change in apoptotic index was detected, but it should be borne in mind that small changes in the rate of apoptosis/cell survival could contribute significantly to tissue growth. From wild type to K:*Igf2*, the crypt number growth rate is only slightly increased, while the PCNA index increases significantly, suggesting that most of the additional cell division goes to turnover. The small increment of net production devoted to growth does, however, produce a considerable cumulative effect over the entire growth phase of the mouse.

Next, we were interested in whether a growth effect arises from a change in size of SPUs, or in the total number of SPUs, or some combination of both. Our results on the colon clearly show that the effect of increased IGF2 is to increase the number of SPUs. There is an increase in crypt length during the maximal growth period, but it is not permanent and does not affect the packing density of crypts in the plane of the epithelium. The number of crypts depends on the rate of crypt fission, and we found that this is accelerated by IGF2 with the main effect being to reduce the duration of crypt fission. The supra-exponential rate of crypt fission is easy to explain under conditions where the majority of the cell production is feeding renewal rather than growth. A small increase in the net proportion devoted to growth will increase the rate of crypt division above the exponential and also shorten the fission time, as observed.

There have been previous studies on the effects of increased cell production on crypt fission (Berlanga-Acosta et al., 2001; Park et al., 1997). Treatment with epidermal growth factor (EGF) increases the labelling index in a similar way to IGF2, but this does not lead to a sustained increase in crypt numbers. Instead there is an early rise and a later fall in crypt fission. Treatment with the mutagen dimethylhydrazine has marginal effects on measured rate of cell production but does increase the fission index, possibly as a regenerative response to tissue damage. These studies concur in identifying the control of crypt division as being separate from the simple production of cells. We also note that a recent study on human colorectal adenomas found an increase in crypt fission, as well as increased crypt height and an expansion of the proliferative zone, precisely the features found in K:*Igf2* colon (Wong et al., 2002). This is of interest, as many colorectal cancers frequently show loss of imprinting (and concomitant overexpression) of IGF2, and IGF2 is the most abundant mRNA overexpressed in colorectal cell lines and tumours (Zhang et al., 1997). The $Apc^{Min/+}$ mutant has a genetic tendency to develop multiple intestinal adenomas. When the K:*Igf2* transgenic line used in this study was crossed to the $Apc^{Min/+}$ mutant, the frequency of colon adenomas was increased 10-fold (Hassan and Howell, 2000). Furthermore, Bjerknes and Cheng have noted the presence of elongated crypts in the 'transitional epithelium' adjacent to adenomas (Bjerknes and Cheng, 1999). This is of interest, as the authors suggest that the adenomas may secrete epithelial trophic factors acting in a paracrine manner to trigger adjacent wild-type crypt enlargement. It is tempting to speculate that IGF2 might be one such trophic factor.

Another aspect of the results is the recognised regional difference in cell kinetics in the colon (Wright and Alison, 1984). We did observe the greatest increase in surface area in the proximal colon, and this is consistent with the effect observed in rat colon when ectopic EGF was administered, suggesting a proximodistal gradient of sensitivity of crypt fission to growth factor stimulation (Ribbons et al., 1994; Park et al., 1997).

It is often not realised that the epidermis of the skin is organised into SPUs. This concept was first advanced by Potten, who studied the cell renewal patterns of epidermis on the dorsal surface of the mouse and proposed that a single stem cell fed each proliferative unit (Potten, 1974). This conception was developed by work of Jones and Watt, who found that stem cells could be identified by integrin immunostaining (Jones et al., 1995). Subsequently, it was supported by cell labelling studies. Mackenzie (Mackenzie, 1997) showed that single *lacZ*-labelled epidermal stem cells would feed a single columnar unit within the epidermis. Likewise, Zhang et al. (Zhang et al., 2001) showed that UV-induced p53 mutant cells will rapidly fill up individual SPUs. Although all these studies support the idea of SPUs fed by a single stem cell, the structure is not in general as regular as that originally described by Potten (see also the irregularity of patches in our Fig. 1B). This means that in the skin we have no simple way of measuring the size of SPUs. However, our data are still consistent with the idea that the mechanism is the same as in the colon, and that excess IGF2 drives a slight increase in the number of cells contributing to growth, which leads to an increase in the number of SPUs and thereby increases the overall area of the skin.

Comparison with *Drosophila*

The most detailed studies of the effects of the insulin/IGF signalling pathway on growth have previously been made in *Drosophila*. Hypomorphic mutation of components of the pathway will decrease overall size, while overexpression will increase overall size. However there is an important difference between the situation in *Drosophila* and in mice, which is that in *Drosophila* a significant component of the effect is on cell size as well as cell number (Stocker and Hafen, 2000). In our case, the difference between the knockout and the wild type is one of SPU number, and therefore also cell number, with conservation of normal cell size. Cell size has also been shown to be normal in the small mouse embryos having *Igf2*-paternal null genotype (Burns and Hassan, 2001). A further difference concerns the issue of disproportion arising from regional

differences in signalling activity. In *Drosophila*, a local increase of signalling in imaginal discs, induced by mitotic recombination, yields clones that themselves may be large and have large cells, but do not affect the overall proportions of the imaginal structure or of the fly as a whole. In our K:*Igf2* mice, a local increase in signalling does cause a local and disproportionate increase in size. The reasons for these differences will require further investigation, but one possibility is that they arise from an absence of an SPU-type of organisation in the imaginal discs.

Because of the general lack of histological analysis and cell kinetic studies of invertebrates, it is hard to say at present whether SPUs are widespread in the animal kingdom or are a specific vertebrate characteristic. Interestingly, vertebrate SPUs are somewhat comparable with the polyps of colonial invertebrates such as hydroids, bryozoa or ascidians (Brusca and Brusca, 1990). Like colonial invertebrates, SPUs can produce new SPUs by budding. It is clear from the present study, as well as others, that budding is not simply a consequence of increased cell production. There must be a level of control that determines whether new cells will feed SPU multiplication or increased cell turnover. The nature of this control remains entirely mysterious. One possibility that has been suggested for small intestinal crypts is that the crucial determinant is the number of stem cells, rather than the total number of dividing cells (Loeffler et al., 1997). If so, this once again points to the factors controlling stem cell identity as a key issue in the control of growth, development and size.

This work was supported by the Medical Research Council and the Association for International Cancer Research. We are grateful to Tia Smith for the epidermal wholemount shown in Fig. 1B, to Patrick Tam (Children's Medical Research Institute, Wentworthville, Australia) for the *H253* mice and to Argiris Efstratiadis (Columbia University, New York) for the *Igf2* knockout mice.

REFERENCES

Berlanga-Acosta, J., Playford, R. J., Mandir, N. and Goodlad, R. A. (2001). Gastrointestinal cell proliferation and crypt fission are separate but complementary means of increasing tissue mass following infusion of epidermal growth factor in rats. *Gut* **48**, 803-807.

Bjerknes, M. (1986). A test of the stochastic theory of stem cell differerentiation. *Biophys. J.* **49**, 1223-1227.

Bjerknes, M. and Cheng, H. (1999). Colossal crypts bordering colon adenomas in Apc(Min) mice express full-length Apc. *Am. J. Pathol.* **154**, 1831-1834.

Brusca, R. C. and Brusca, G. J. (1990). *Invertebrates*. Sunderland, MA: Sinauer Associates Inc.

Burns, J. L. and Hassan, A. B. (2001). Cell survival and proliferation are modified by insulin-like growth factor 2 between days 9 and 10 of mouse gestation. *Development* **128**, 3819-3830.

Cairnie, A. B. and Millen, B. H. (1975). Fission of crypts in the small intestine of the irradiated mouse. *Cell Tiss. Kinet.* **8**, 189-196.

Canter, C. E. and Goss, R. J. (1975). Induction of extra nephrons in unilaterally nephrectomized immature rats. *Proc. Soc. Exp. Biol. Med.* **148**, 294-296.

Cheng, H. and Bjerknes, M. (1985). Whole population cell kinetics and postnatal development of the mouse intestinal epithelium. *Anat. Rec.* **211**, 420-426.

Christofori, G., Naik, P. and Hanahan, D. (1995). Deregulation of both imprinted and expressed alleles of the insulin-like growth factor 2 gene during β-cell tumorigenesis. *Nat. Genet*, **10**: 196-201.

De Chiara, T., Efstratiadis, A. and Robertson, E. (1990). A growth-deficiency phenotype in heterozygous mice carrying an insulin-like growth factor-ii gene disrupted by targeting. *Nature* **345**, 78-80.

Efstratiadis, A. (1998). Genetics of mouse growth. *Int. J. Dev. Biol.* **42**, 955-976.

Ezaki, T. (2000). Antigen retrieval on formaldehyde-fixed paraffin sections: its potential drawbacks and optimization for double immunostaining. *Micron* **31**, 639-649.

Goodlad, R. A. (1994). Microdissection-based techniques for the determination of cell proliferation in gastrointestinal epithelium: application to animal and human studies. In *Cell Biology: A Laboratory Handbook*. (ed. J. E. Celis), pp. 205-216. London: Academic Press.

Gordon, J. I., Schmidt, G. H. and Roth, K. A. (1992). Studies of intestinal stem cells using normal, chimeric and transgenic mice. *FASEB J.* **6**, 3039-3050.

Goss, R. J. (1972). *Regulation of Organ and Tissue Growth*. New York, London: Academic Press.

Hassan, A. B. and Howell, J. A. (2000). Insulin-like growth factor II supply modifies growth of intestinal adenoma in Apc(Min/+) mice. *Cancer Res.* **60**, 1070-1076.

Jiang, X., Hitchcock, A., Bryan, E. J., Watson, R. H., Englefield, P., Thomas, E. J. and Campbell, I. G. (1996). Microsatellite analysis of endometriosis reveals loss of heterozygosity at candidate ovarian tumor suppressor gene loci. *Cancer Res.* **56**, 3534-3539.

Jones, P. H., Harper, S. and Watt, F. M. (1995). Stem cell patterning and fate in human epidermis. *Cell* **80**, 83-93.

Leevers, S. J. (2001). Growth control: invertebrate surprises. *Curr. Biol.* **11**, R209-R212.

Loeffler, M., Bratke, T., Paulus, U., Li, Y. Q. and Potten, C. S. (1997). Clonality and life cycles of intestinal crypts explained by a state dependent model of epithelial stem cell organization. *J. Theor. Biol.* **186**, 41-54.

Lyon, M. F. (1961). Gene action in the X chromosome of the mouse (Mus Musculus L.). *Nature* **190**, 370-373.

Mackenzie, I. C. (1997). Retroviral transduction of murine epidermal stem cells demonstrates clonal units of epidermal structure. *J. Invest. Dermatol.* **109**, 377-383.

Maskens, A. P. (1978). Histogenesis of colon glands during postnatal growth. *Acta Anatomica* **100**, 17-26.

Oldham, S., Bohni, R., Stocker, H., Brogiolo, W. and Hafen, E. (2000). Genetic control of size in Drosophila. *Philos. Trans. R. Soc.* **355**, 945-952.

Park, H. S., Goodlad, R. A., Ahnen, D. J., Winnett, A., Sasieni, P., Lee, C. Y. and Wright, N. A. (1997). Effects of epidermal growth factor and dimethylhydrazine on crypt size, cell proliferation, and crypt fission in the rat colon. *Am. J. Pathol.* **151**, 843-852.

Petrik, J., Pell, J. M., Arany, E., McDonald, T. J., Dean, W. L., Reik, W. and Hill, D. J. (1999). Overexpression of insulin-like growth factor-II in transgenic mice is associated with pancreatic islet cell hyperplasia. *Endocrinology* **140**, 2353-2363.

Ponder, B. A. J., Schmidt, G. H., Wilkinson, M. M., Wood, M. J., Monk, M. and Reid, A. (1985). Derivation of mouse intestinal crypts from single progenitor cells. *Nature* **313**, 689-691.

Potten, C. S. (1974). The epidermal proliferative unit: the possible role of the central basal cell. *Cell Tiss. Kinet.* **1**, 77-88.

Potten, C. S. (1978). Epithelial proliferative subpopulations. In *Stem Cells and Tissue Homeostasis* (ed. B. I. Lord, C. S. Potten and R. J. Cole), pp. 317-334. Cambridge: Cambridge University Press.

Potten, C. S. (1998). Stem cells in gastrointestinal epithelium: numbers, characteristics and death. *Philos. Trans. R. Soc. Lond. Ser. B Biol. Sci.* **353**, 821-830.

Potten, C. S. and Grant, H. K. (1998). The relationship between ionizing radiation-induced apoptosis and stem cells in the small and large intestine. *Br. J. Cancer* **78**, 993-1003.

Raff, M. C. (1996). Size control: the regulation of cell numbers in animal development. *Cell* **86**, 173-175.

Ribbons, K. A., Howarth, G. S., Davey, K. B., Georgenascimento, C. and Read, L. C. (1994). Subcutaneous but not intraluminal epidermal growth-factor stimulates colonic growth in normal adult-rats. *Growth Factors* **10**, 153-162.

Schmidt, G. H., Winton, D. J. and Ponder, B. A. J. (1988). Development of the pattern of cell renewal in the crypt-villus unit of chimaeric mouse small intestine. *Development* **103**, 785-790.

Slack, J. M. W. (1996). The mysterious mechanism of growth. *Curr. Biol.* **6**, 348.

Smith, J., Goldsmith, C., Ward, A. and LeDieu, R. (2000). IGF-II

ameliorates the dystrophic phenotype and coordinately down-regulates programmed cell death. *Cell Death Diff.* **7**, 1109-1118.

Stocker, H. and Hafen, E. (2000). Genetic control of cell size. *Curr. Opin. Genet. Dev.* **10**, 529-535.

Tan, S. S., Williams, E. A. and Tam, P. P. L. (1993). X-chromosome inactivation occurs at different times in different tissues of the post implantation mouse embryo. *Nat. Genet.* **3**, 170-174.

Tsai, Y. C., Lu, Y., W, N. P., Zlotnikov, G., Jones, P. A. and Smith, H. S. (1996). Contiguous patches of normal human mammary epithelium derived from a single stem cell: Implications for breast carcinogenesis. *Cancer Res.* **56**, 402-404.

Ward, A. (1997). Beckwith-Wiedemann syndrome and Wilms' tumour. *Mol. Hum. Reprod.* **3**, 157-168.

Ward, A., Bates, P., Fisher, R., Richardson, L. and Graham, C. F. (1994). Disproportionate growth in mice with Igf-2 transgenes. *Proc. Natl. Acad. Sci. USA* **91**, 10365-10369.

Ward, A., Fisher, R., Richardson, L., Pooler, J.-A., Squire, S., Bates, P., Shaposhnikov, R., Hayward, N., Thurston, M. and Graham, C. F. (1997). Genomic regions regulating imprinting and insulin-like growth factor-II promoter 3 activity in transgenics: novel enhancer and silencer elements. *Genes Funct.* **1**, 25-36.

Watt, F. M. (1998). Epidermal stem cells: markers, patterning and the control of stem cell fate. *Phil. Trans. R. Soc. B* **353**, 831-837.

Weinberg, W. C., Howard, J. C. and Iannaccone, P. (1985). Histological demonstration of mosaicism in a series of chimeric rats produced between congenic strains. *Science* **227**, 524-527.

Winton, D. J., Blount, M. A. and Ponder, B. A. J. (1988). A clonal marker induced by mutation in mouse intestinal epithelium. *Nature* **333**, 463-466.

Wong, W. M., Mandir, N., Goodlad, R. A., Wong, B. C. Y., Garcia, S. B., Lam, S. K. and Wright, N. A. (2002). Histogenesis of human colorectal adenomas and hyperplastic polyps: the role of cell proliferation and crypt fission. *Gut* **50**, 212-217.

Wright, N. A. and Alison, M. (1984). *The Biology of Epithelial Cell Populations*, Vols 1 and 2. Oxford: Clarendon Press.

Zhang, L., Zhou, W., Velculescu, V. E., Kern, S. E., Hruban, R. H., Hamilton, S. R., Vogelstein, B. and Kinzler, K. W. (1997). Gene expression profiles in normal and cancer cells. *Science* **276**, 1268-1272.

Zhang, W. G., Remenyik, E., Zelterman, D., Brash, D. E. and Wikonkal, N. M. (2001). Escaping the stem cell compartment: Sustained UVB exposure allows p53-mutant keratinocytes to colonize adjacent epidermal proliferating units without incurring additional mutations. *Proc. Natl. Acad. Sci. USA* **98**, 13948-13953.